Research Article

Hussein Hayder Mohammed Ali, Ali Jasim Mohammed, Mohammed J. Alshukri*, Adnan M. Hussien and Ammar I. Alsabery

Numerical study on entropy minimization in pipes with helical airfoil and CuO nanoparticle integration

https://doi.org/10.1515/eng-2022-0594 received September 05, 2023; accepted January 30, 2024

Abstract: In this study, minimizing entropy generation in a horizontal pipe is numerically investigated through two passive techniques: in the first mode, the helical wire inserts in the pipe were placed at three various ratios of pitch ratio. The second mode is adding cupric oxide nanoparticles at various volume concentrations. Experiments were conducted for Reynolds numbers ranging from 4,000 to 14,000 under a uniform heat flux scenario of 25,000 W/m². The study utilized the ANSYS 14.5 software, employing the K-omega standard model, which involves three primary governing equations: continuity, momentum, and energy. According to the data, it was determined that the helical wire placed inside the pipe with a small pitch ratio decreased the entropy generation number. Cupric oxide nanoparticles also have a substantial impact on the entropy generation number. The higher volume concentration models had lower entropy generation numbers and Bejan numbers than the other models. Comparative analyses further emphasize the substantial advantages of using cupric oxide nanofluids and helical-wire inserts, with efficiency gains ranging from 5.08 to 11.7%.

Keywords: entropy generation, numerical investigation, nanofluids, helical airfoil, Bejan numbers

Nomenclature

\boldsymbol{A}	cross-sectional area (m²)
D	inner diameter of the tube (m)
f	friction factor
h	heat transfer coefficient (W/m² K)
k	thermal conductivity (W/mK)
L	length of the tube (m)
$N_{\rm s}$	entropy generation number
$S_{\rm gen}'$	entropy generation rate
m	air mass flow rate (kg/s)
P.R	pitch ratio of helical wire (m)
Pr	Prandtl number
Nu	Nusselt number
Q	heat transfer (W)
q'	heat flux (W/m²)
Re	Reynolds number (UD/v)
T	steady state temperature (K)
ΔP	pressure drop (Pa)

volumetric flow rate (m³/s)

Greek letters

ρ	fluid density (kg/m³)
ν	kinematic viscosity (m³/s)
μ	dynamic viscosity (kg/ms)
Ø	concentration

^{*} Corresponding author: Mohammed J. Alshukri, Department of Mechanical Engineering, Faculty of Engineering, Kufa University, 54002, Najaf, Iraq, e-mail: mohammedj.alshukry@uokufa.edu.iq
Hussein Hayder Mohammed Ali, Ali Jasim Mohammed, Adnan M.
Hussien: Department of Mechanical Power Techniques Engineering, Northern Technical University, Technical College, 36001, Kirkuk, Iraq
Ammar I. Alsabery: Refrigeration & Air-conditioning Technical
Engineering Department, College of Technical Engineering, The Islamic University, Najaf, Iraq

Subscripts

nf	nanofluid	
S	solid	
W	water	
i	inlet	
0	outlet	

1 Introduction

Due to the scarcity of energy sources, energy conservation has become a primary concern in thermodynamic systems. The method of "heat transfer enhancement" employs both active and passive techniques to expedite heat transfer in thermal systems. Various strategies are employed in different heat exchanger applications to enhance efficiency. Heat exchangers find extensive use in thermal systems, including central heating, air conditioning, and various chemical industrial processes. Eddy current components like twisted tapes, coiled wires, vortex generators, and vortex and conical rings have been developed to enhance the thermohydraulic efficiency of heat exchangers by incorporating nanofluids. An intriguing approach involves surface roughening with helical and transverse ribs, akin to coiled wire inlays [1]. The insertion of coiled wire significantly disrupts boundary layers, promoting the reconstruction of hydrodynamic, thermal, and boundary layers within the pipe's flow. Moreover, with helically coiled wires, secondary flow can be generated, accelerating the heat transfer rate by enhancing vortex formation in turbulence.

Exergy analyses and the reduction of entropy generation through passive heat transfer enhancement methods have been extensively studied theoretically, analytically, and experimentally. Employing numerical methods, Ko and Wu [2] delved into entropy production caused by turbulence-forced convection in a curved rectangular channel with external heating. They identified two sources of entropy generation: frictional irreversibility near duct walls and heat transfer irreversibility near the outer wall, which receives external heat flux. You et al. [3] scrutinized the laminar thermal augmentation of horizontal circular tubes with conical strip inserts, focusing on minimizing entropy generation. Results showed that non-staggered strips performed better than staggered ones, exhibiting higher entropy generation rates. In a separate investigation, Mwesigye et al. [4] conducted a numerical evaluation of heat transfer and entropy generation using a parabolic trough receiver with wall-removable twisted tape inserts. The findings demonstrated that using twisted tape inserts at lower Reynolds numbers significantly decreased the rate of entropy production.

Siavashi et al. [5] quantitatively analyzed natural convection throughout a square container, incorporating a porous medium supplied with fluid. They determined that situation (a), which was more successful, represented the best design, as it generated the least amount of entropy. In a related study, Farzaneh-Gord et al. [6] explored the optimal construction and functional conditions for inclined tube heat exchangers in both turbulent and laminar flows. It was found that optimizing the efficiency of this type of heat

exchanger involved employing the minimum rate of entropy formation.

A number of studies have evaluated entropy evolution while using nanofluids as working fluids. Chen and Liu [7] performed a numerical analysis of entropy generation in a fully developed mixed convective Al₂O₃-water nanofluid in a channel. The findings showed that the average entropy generation number of nanofluid is lower than that of pure water. In a tube submerged in an isothermal external fluid, Anand [8] investigated the calculation of entropy generation induced by nanofluid flow. It was found that the rate of entropy formation decreased as the heat transfer rate increased. Huminic and Huminic [9] used two different types of nanofluids to investigate the thermal performance and entropy generation in the spirally wound pipes of tubular heat exchangers in the regime of laminar flow. Entropy is generated less frequently as the volume concentration of nanoparticles increases. Ebrahimi et al. [10] investigated entropy generation in microchannels utilizing longitudinal vortex generators and nanofluids with different Revnolds numbers. The results showed that using nanofluids as working fluids reduced the degree of irreversibility of rectangular microchannels. For both turbulent and laminar modes, Moghaddami et al. [11] conducted a study to investigate how nanoparticle incorporation affects the formation of entropy in water-Al₂O₃ nanofluids flowing in a circular conduit with a thermal boundary condition of constant wall heat flux. The introduction of nanoparticles enhances entropy formation whenever fluid flow (pressure drop) exhibits a high degree of irreversibility. Keklikcioglu and Ozceyhan [12] conducted a study on entropy generation within a circular pipe equipped with a tightly coiled insert. The insert featured equilateral triangular cross-section wires with their edges aligned in the flow direction. The entropy generation number increased with higher Reynolds numbers and decreased with greater pitch ratios. In comparison to alternative systems, co-generation with narrower wires exhibited a lower entropy generation rate.

As previously mentioned, the presence of nanoparticles enhances fluid heat transfer qualities while simultaneously increasing fluid flow pressure drop. The elevated pressure drop results in irreversibility and energy loss within the system, but the improved heat transfer properties limit entropy generation and irreversibility. Bejan's concept of minimizing entropy generation [13] suggests that the optimal state for a thermal system is achieved when entropy generation is reduced. In other words, the ideal design for a heat exchanger considers how to enhance heat transfer efficiency while minimizing pressure drop.

Since no prior research has presented an analysis of entropy generation for a tube equipped with helical airfoil

(0030) cross-sectional coiled wire inserts, the current study employs numerical methods to assess entropy generation in such a configuration for CuO/water nanofluid flow. The airfoil-shaped wire induces flow expansion near the wall, significantly accelerating boundary layer breakdown. The research aims to identify the optimal design and conditions for minimizing entropy generation and promoting faster heat transfer rates in nanofluid flow by disrupting the laminar boundary layer.

2 Material and method

2.1 Numerical method

In this study, numerical analyses were carried out by applying the finite volume method in ANSYS Fluent 14.5. A single-phase model was identified as a flow condition of nanoparticles with base fluid. The k-omega standard model was chosen as the turbulence model. The relationship between pressure and velocity was evaluated using the SIMPLIC algorithm. To analyze the heat transfer, the komega standard model uses three governing equations: continuity, momentum, and energy, and these are given in equations (1)–(3), respectively [14–16].

Continuity equation:

$$\nabla \cdot (\rho_{\rm m} \vec{v}_{\rm m}) = 0. \tag{1}$$

Momentum equation

$$\nabla \cdot (\rho_{\mathbf{m}} \overrightarrow{v_{\mathbf{m}}} \overrightarrow{v_{\mathbf{m}}}) = -\nabla P + \nabla \cdot [\mu_{\mathbf{m}} (\nabla \overrightarrow{v_{\mathbf{m}}} + \nabla \overrightarrow{v_{\mathbf{m}}}^{\mathrm{T}})] + \nabla \cdot \left[\sum_{k=1}^{n} \emptyset_{k} \rho_{k} \overrightarrow{v_{\mathbf{d}r_{,k}}} \overrightarrow{v_{\mathbf{d}r_{,k}}} \right].$$
(2)

Energy equation

$$\nabla \cdot \sum_{k=1}^{n} (\emptyset k \ \overrightarrow{v}_{k}(\rho_{k} \ h_{k} + p)) = \nabla \cdot (k_{\text{eff}} \nabla T). \tag{3}$$

2.2 Numerical model and boundary conditions

In this quantitative study, experiments were carried out using the Computational Fluid Dynamics method for the 3D pipe with a helical airfoil (0030) cross-sectional area inserted inside the test section as depicted in Figure 1. The Solidworks program designed the geometric model, which consisted of a straight pipe 40 mm in diameter. There were three

primary portions to the pipe. To maintain a fully developed flow through the pipe, the intake section should be 10D (about 400 mm), the test section should be 5D (about 1,000 mm), and the outflow portion should be 200 mm (5D) to prevent the influence of backflow at the fluid outlet. For four tested nanoparticle volume concentrations of 0.15, 0.39, 1, and 2%, the Reynolds numbers have ranged from 4,000 to 14,000.

2.2.1 Independence of grid

Rashidi et al. [17] highlight that numerical methods involve estimation alongside experimental techniques, incorporating error rates. It is ensured grid independence in the numerical model is vital for assessing the study's conclusions accurately. Various mesh types undergo separate testing, observing related components' values with comparable or identical Nusselt numbers. The selected grid arrangement and cell size within the flow area are illustrated in Figure 2.

2.2.2 Thermophysical properties of nanofluids

Nanofluids can be thought of as single substances rather than mixtures [18]. It has been shown that nanofluids have superior thermophysical characteristics compared to basic liquids. The following equations are provided for finding the thermophysical characteristics of nanofluids [19]:

$$\rho_{\rm nf} = \emptyset \times \rho_{\rm s} + (1 - \emptyset) \times \rho_{\rm w}, \tag{4}$$

$$C_{\text{pnf}} = \frac{\varnothing \times (\rho_{\text{s}} \times c_{\text{ps}}) + (1 - \varnothing) \times (\rho_{\text{w}} \times C_{\text{pw}})}{\rho_{\text{nf}}}, \quad (5)$$

$$K_{\rm nf} = \left[\frac{k_{\rm s} + 2k_{\rm w} + 2 \times (k_{\rm s} - k_{\rm w}) \times (1 + \beta)^3 \times \emptyset}{k_{\rm s} + 2k_{\rm w} - (k_{\rm s} - k_{\rm w}) \times (1 + \beta)^3 \times \emptyset} \right] \times k_{\rm w} \text{ where } \beta = 0.1,$$
(6)

$$\mu_{\rm nf} = \mu_{\rm w} \times (1 + 2.5 \times \varnothing). \tag{7}$$

The thermophysical properties of CuO and water used in the computation of the thermophysical properties of nanofluids are summarized in Table 1 [20,21].

Table 1: Thermo-physical properties of water and CuO

	k (W/m °C)	Cp (J/kg °C)	ρ (kg/m³)
Water	0.589	4,185	999.1
CuO	69	535.6	6,350

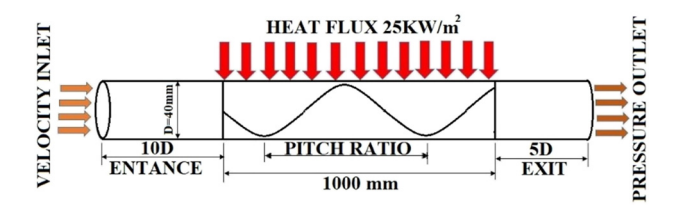


Figure 1: The boundary conditions for test pipe.

2.2.3 Calculation method

After determining the physical properties of the nanofluid, it was submitted to the ANSYS 14.5 software for analysis. According to the results of the analysis, the values of the Reynolds number, heat transfer coefficient, friction factor, entropy generation, Nusselt number, dimensionless entropy generation number, and the Bejan number were obtained according to the subsequent equations, respectively [12].

$$Re = \frac{\rho \times \nu \times d}{\mu},$$
 (8)

$$h = \frac{q'}{T_{\rm S} - T_{\rm b}},\tag{9}$$

$$Nu = \frac{h \times d}{k}, \tag{10}$$

$$f = \frac{\Delta P}{\frac{L}{2D}\rho V^2},\tag{11}$$

$$S'_{\text{gen}} = \frac{q'^2}{\pi T^2 k \text{Nu}} + \frac{32m^3 f}{\pi^2 o^2 T D^5}.$$
 (12)

Straight pipe may be calculated using the above formula. It can be utilized for helical wires and nanofluidic streamline inserts, however. The consequences of heat transmission are described in the equation's first part, while fluid friction is discussed in the second term.

To assess the practical impact of heat transfer enhancement methods on the thermodynamic performance of a heat exchanger, it is essential to compare the entropy generation rates before and after improvement. This evaluation is conducted using the entropy production number (N_s) , as defined by equation (13).

$$N_{\rm S} = \frac{S_{\rm gen,n}'}{S_{\rm gen,s}'}.$$
 (13)

Heat transfer enhancement methods using $N_s < 1$ are thermodynamically beneficial, as these methods reduce the amount of irreversible unit performance and improve the heat transfer rate [22].

In this study, the Bejan number, a dimensionless number, is used to evaluate the performance of a thermal system in terms of entropy generation. It denotes the proportion of irreversibility caused by heat transfer to overall irreversibility. As given by the equation [23]:

Be =
$$\frac{\dot{S}'_{\text{gen},\Delta T}}{\dot{S}'_{\text{gen},\Delta T} + \dot{S}'_{\text{gen},\Delta P}}.$$
 (14)

The Bejan number has a value range of 0–1. When the Bejan number approaches 1, heat transfer irreversibilities are said to be greater than total fluid friction irreversibilities.

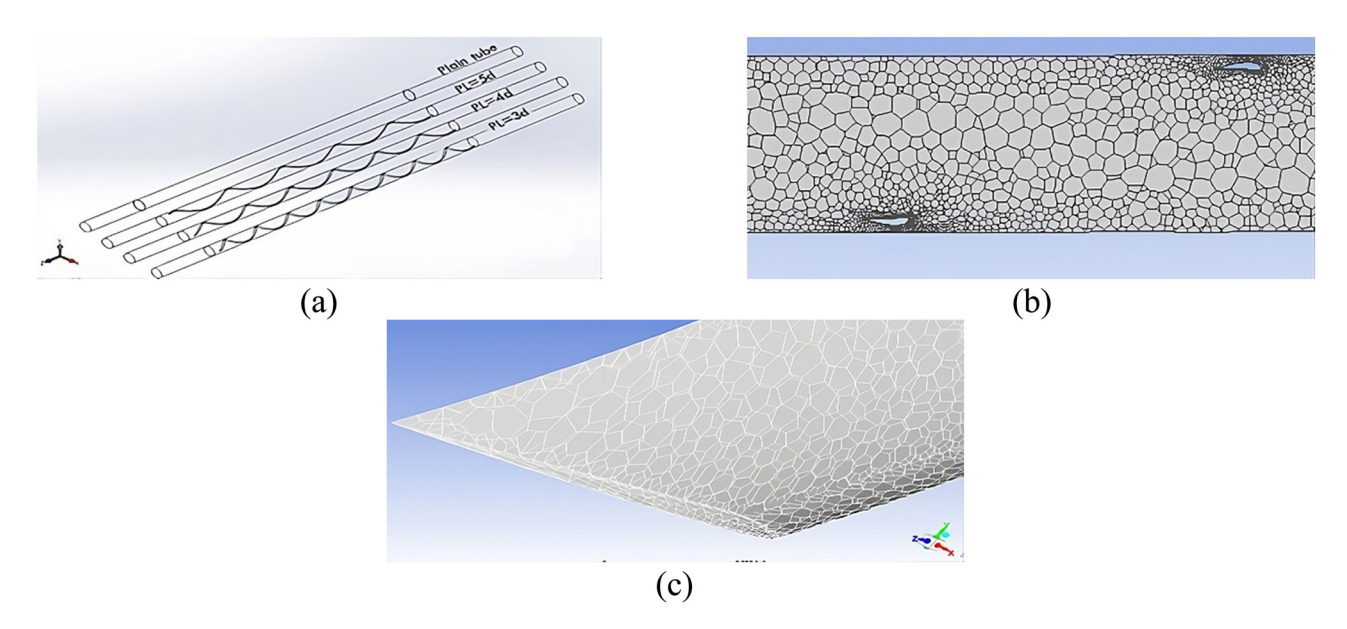


Figure 2: Schematic of the pipe with the helical airfoil: (a) pipes with helical airfoil, (b) pipe's longitudinal section with helical airfoil mesh, and (c) airfoil mesh.

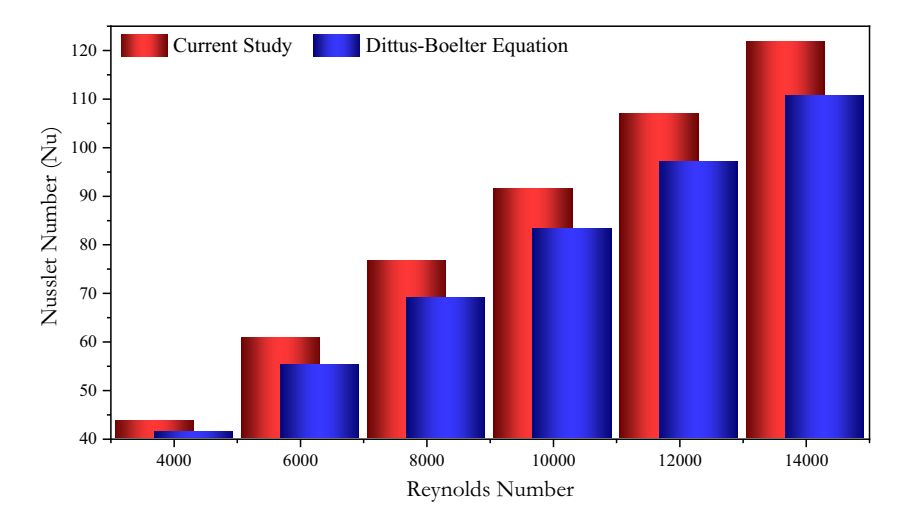


Figure 3: Comparison between the Nusselt number of the present study and the Dittus-Boelter equation.

3 Results and discussion

3.1 Validation of numerical study

The findings of numerical research should be compared to well-known relationships, and the study should be validated. In this research, the findings of an analysis utilizing just base fluid water were compared to the Dittus-Boelter and Blasius [23] equations for the Nusselt number and friction factor, which are provided in equations (15) and (16), respectively.

$$Nu = 0.023 \, Re^{0.8} \, Pr^{0.4}, \tag{15}$$

$$f = 0.316 \,\mathrm{Re}^{-0.25}$$
 (16)

Both the Nusselt number and the friction factor were compared to well-known correlations in the literature, as shown in Figures 3 and 4. It was discovered that the numerical research findings at various Reynolds numbers and the values derived from well-known correlations are almost identical and follow the same pattern. For the Nusselt number and the friction factor, the greatest deviations between numerical findings and correlation values were $\pm 3-6\%$ and $\pm 1-7\%$, respectively.

3.2 Analysis of the generation of entropy

3.2.1 Entropy generation number

In the exploration of heat exchangers' heat transfer and pressure drop characteristics, a diverse range of fluids can be employed. However, for a comprehensive assessment

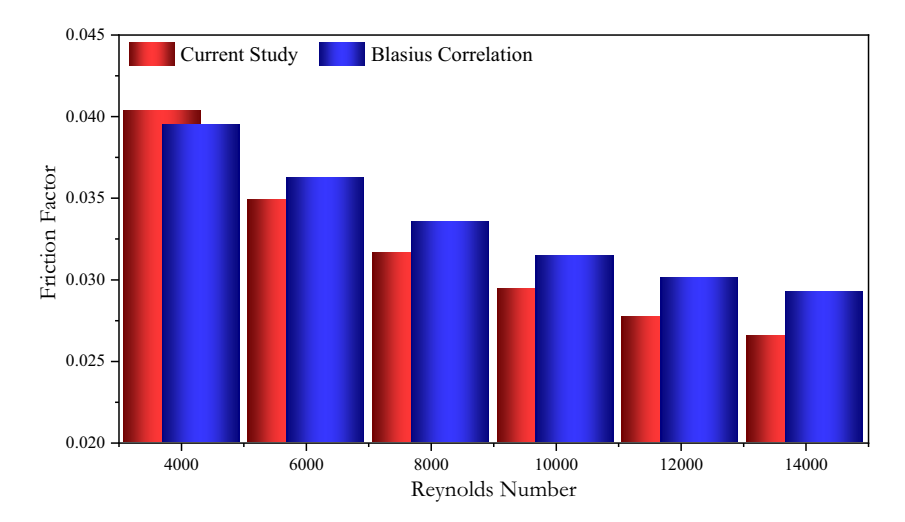


Figure 4: Comparison of the friction factor between the present study with Blasius correlation.

of the system's performance, entropy generation values before and after applying augmentation techniques need to be compared to evaluate both fluid and thermodynamic effectiveness. This is vital for gaining a holistic understanding of the thermal system's behavior.

This study focuses on the assessment of tubular heat exchangers utilizing nanofluids, with a particular emphasis on investigating the entropy generation principle in pipes featuring helical wing (0030) inserts. The primary objective is to uncover the impact of these inserts on entropy generation. The helical airfoil inserts stimulate the redevelopment of thermal and hydrodynamic boundary layers, inducing vorticity and irreversibility in the flow, consequently leading to increased entropy production within the pipe. This, in turn, restricts the thermodynamic benefits of the system due to the ascending trend of entropy generation.

In Figure 5(a–c), entropy generation numbers are depicted for various Reynolds numbers (4,000–14,000) and four-volume concentrations of CuO nanofluids (0.15, 0.39, 1, and 2% by volume fractions) at different pitch ratios (P.R. = 3D, 4D, and 5D). Notably, as the Reynolds number increases, the entropy generation number diminishes. Volume concentrations also influence the rate of entropy formation, showing a decreasing trend with higher concentrations. An

essential criterion for thermal system effectiveness is an entropy production number smaller than unity. The comparisons in Figure 5(a)–(c) highlight significant observations. The entropy generation number of water only at (Re = 14,000) increases by 11.7% when comparing Figure 5(c) with Figure 5(a). Similar comparisons indicate an increase of 7% when compared with Figure 5(b), and an increase of 5.56% for mode water only compared with mode (\emptyset = 2%) in Figure 5(c). Further increases of 5.08, 5.23, and 5.39% are observed when comparing mode number water only with mode numbers (\emptyset = 0.15%), (\emptyset = 0.39%), and (\emptyset = 1%), respectively.

In conclusion, the investigation delves into entropy generation within tubular heat exchangers employing helical wing inserts, revealing intricate dynamics that influence the thermodynamic behavior of the system. The detailed insights from this analysis contribute to a more comprehensive understanding of heat exchanger performance.

3.2.2 Thermal entropy generation

The thermal entropy generation for different Reynolds numbers with different pitch ratios (P.R = 3D, 4D, and 5D) at various volume concentrations (\varnothing = 0, 0.15, 0.39, 1, and 2%) of CuO

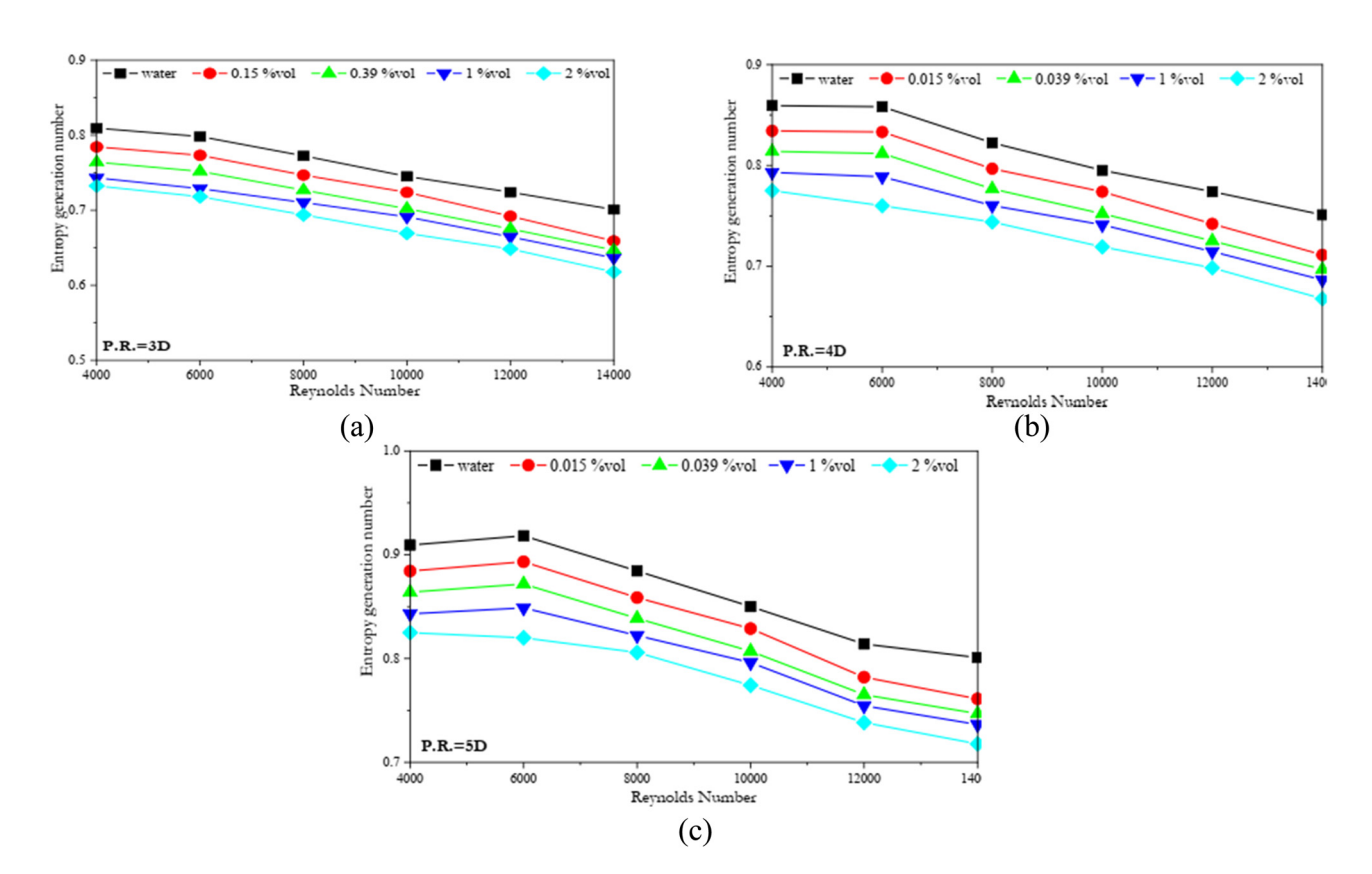


Figure 5: Entropy generation number versus Reynolds number for various volume concentrations at (a) P.R. = 3D (b) P.R. = 4D, and (c) P.R. = 5D.

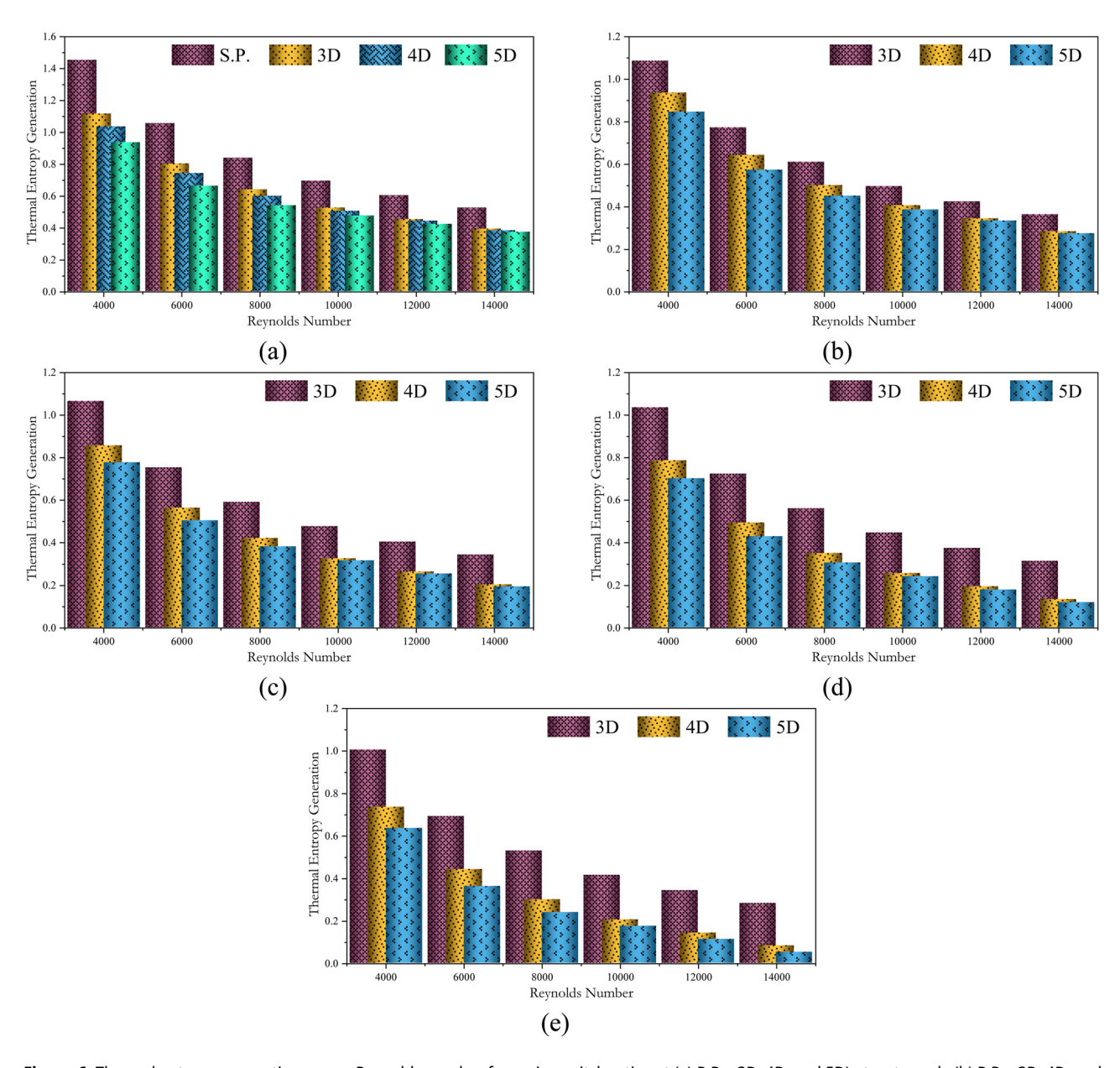


Figure 6: Thermal entropy generation versus Reynolds number for various pitch ratios at (a) P.R = 3D, 4D, and 5D) at water only (b) P.R = 3D, 4D, and 5D with \emptyset = 0.15, (c) P.R = 3D, 4D, and 5D with \emptyset = 0.39, (d) P.R = 3D, 4D, and 5D with \emptyset = 1, and (e) P.R = 3D, 4D, and 5D with \emptyset = 2.

nanofluids is shown in Figure 6(a-e). As the Reynolds number and pitch ratios of the nanofluid rise, the thermal entropy generation decreases. Increased particle loading speeds improve system performance while lowering the thermal entropy generation number. The thermal entropy production rises slowly with the increase in pitch ratios due to the rising trend of frictional irreversibility and turbulent intensity. As the volume concentration of the nanofluid rises, the thermal entropy generation decreases due to the improved thermal and physical properties of the nanofluid.

3.2.3 Frictional entropy generation

In Figure 7(a), the relationship between frictional entropy generation and Reynolds number is depicted for various pitch ratios (P.R = 3D, 4D, and 5D) in water alone. This illustration reveals that pitch ratios contribute to an increase in the rate of frictional entropy generation, attributed to fluid friction with the twist tape, and conversely, an escalation in thermal entropy generation. Upon comparing Figure 7(e) with Figure 7(a-d), a notable reduction in the frictional entropy generation rate is observed due to the volume concentration of the nanofluid,

while the thermal entropy generation experiences an upturn owing to the enhanced physical properties of the nanofluid.

3.2.4 Bejan number

Another dimensionless number to consider when analyzing entropy generation in thermal systems is the

Bejan number. As the pitch ratio of the helical insertion increased, the Bejan number grew, as shown in Figure 8(a–e). At high Reynolds numbers, frictional irreversibility trumped heat transfer irreversibility. Also, it was clear that the higher volume concentration models had lower entropy generation numbers and Bejan numbers than the other models.

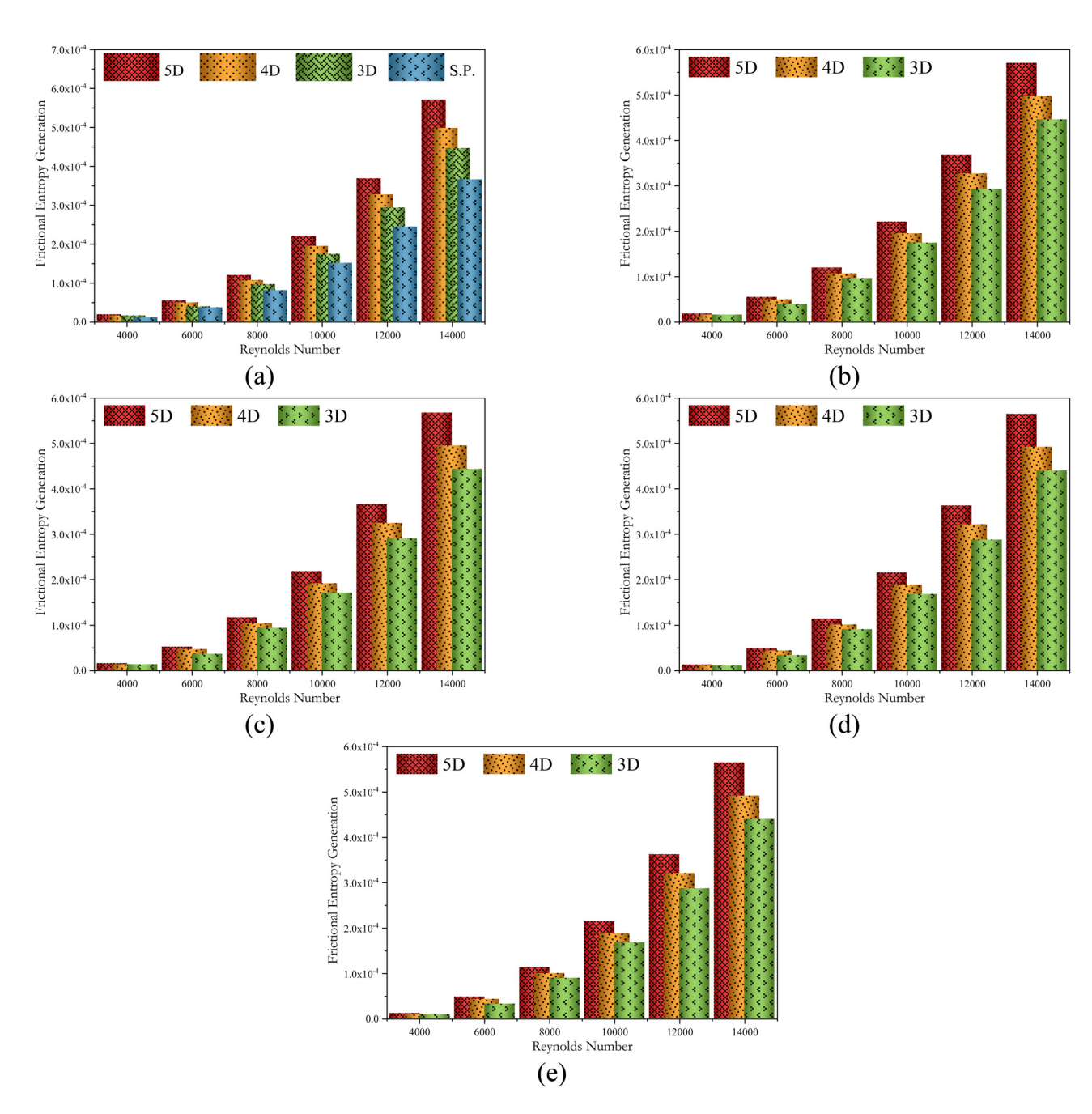


Figure 7: Frictional entropy generation versus Reynolds number for various pitch ratios at (a) P.R = 3D, 4D, and 5D) at water only; (b) P.R = 3D, 4D, and 5D with \emptyset = 0.15; (c) P.R = 3D, 4D, and 5D with \emptyset = 0.39; (d) P.R = 3D, 4D, and 5D with \emptyset = 1; and (e) P.R = 3D, 4D, and 5D with \emptyset = 2.

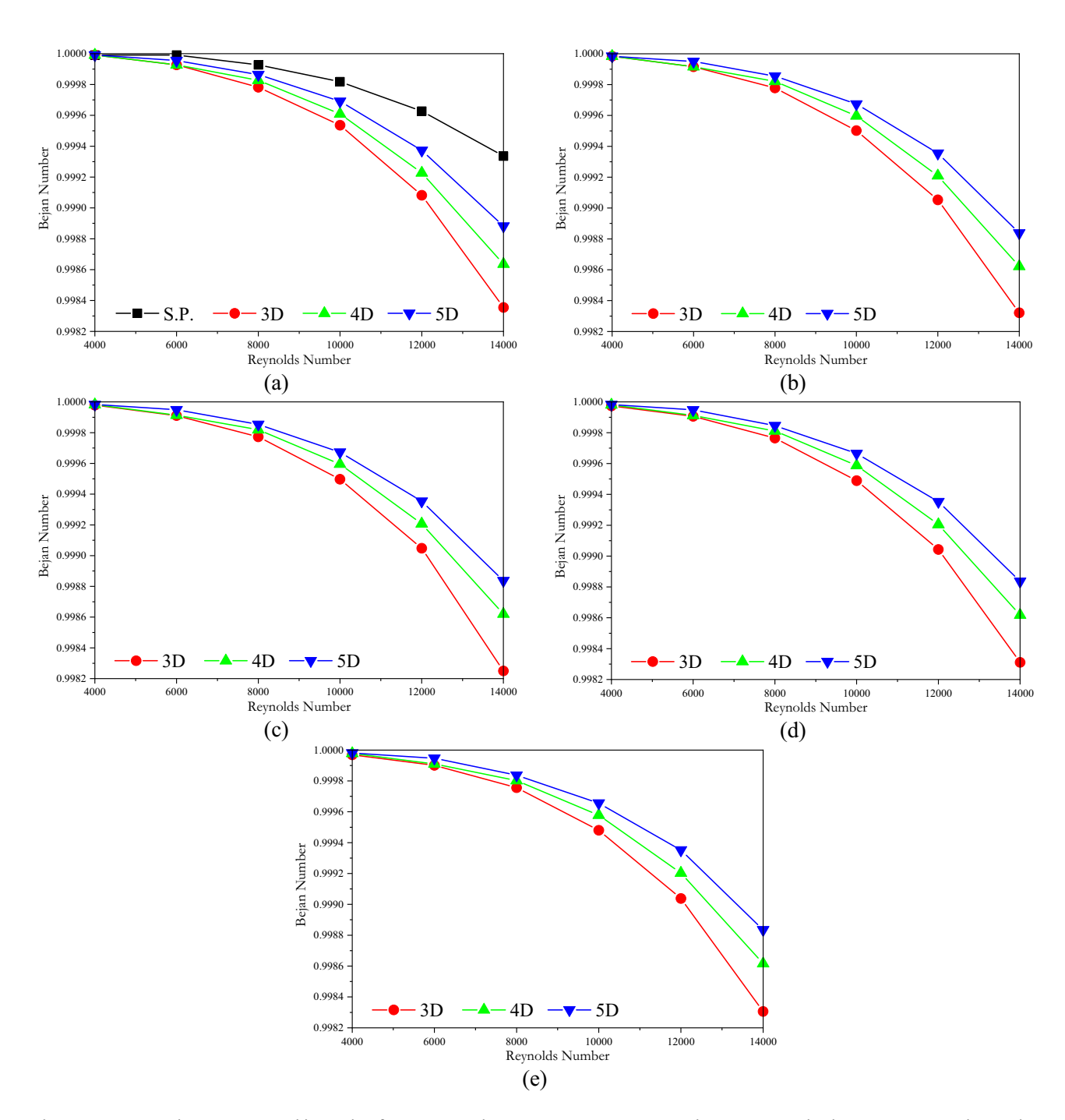


Figure 8: Bejan number versus Reynolds number for various pitch ratios at (a) P.R = 3D, 4D, and 5D at water only; (b) P.R = 3D, 4D, and 5D with \varnothing = 0.15; (c) P.R = 3D, 4D, and 5D with \varnothing = 0.39; (d) P.R = 3D, 4D, and 5D with \varnothing = 1; and (e) P.R = 3D, 4D, and 5D with \varnothing = 2.

4 Conclusion

In conclusion, this study has provided a comprehensive quantitative analysis of entropy generation in a horizontally oriented circular tube equipped with airfoil cross-sectioned helical-wire inserts. The investigation encompassed a diverse range of Reynolds numbers, from 4,000 to 14,000, and examined the influence of various parameters, including airfoil

selection and pitch-to-diameter ratios (P.R = 3, 4, and 5). The findings highlighted a direct relationship between Reynolds number and entropy generation, indicating the significance of fluid flow conditions in shaping system behavior. Moreover, smaller pitches for helical-wire inserts were observed to effectively reduce entropy generation, leading to enhanced thermodynamic efficiency.

Notably, the presence of CuO nanoparticles significantly impacted entropy generation behavior. The study's results reveal that higher Reynolds numbers lead to a reduction in entropy generation, indicating enhanced thermal system performance. Additionally, an increase in the volume concentration of CuO nanofluids corresponds to a decrease in entropy production, thus improving system efficiency. A crucial criterion for effective thermal systems is an entropy production number below unity. Comparative analyses further emphasize the substantial advantages of using CuO nanofluids and helical-wire inserts, with efficiency gains ranging from 5.08 to 11.7%. So, increased volume concentrations of CuO nanoparticles corresponded to decreased entropy generation numbers and Bejan numbers, revealing the interplay between nanoparticle characteristics and system performance. This research contributes valuable insights into the intricate dynamics of entropy generation within heat exchangers featuring helical-wire inserts. The comprehensive analysis of multiple parameters provides a deeper understanding of thermodynamic optimization and system performance enhancement.

Funding information: Authors declare that the manuscript was done depending on the personal effort of the author, and there is no funding effort from any side or organization.

Conflict of interest: The authors state no conflict of interest.

Data availability statement: Most data sets generated and analyzed in this study are comprised in this submitted manuscript. The other data sets are available on reasonable request from the corresponding author with the attached information.

References

- [1] Ravigururajan T, Bergles A. Development and verification of general correlations for pressure drop and heat transfer in single-phase turbulent flow in enhanced tubes. Exp Therm Fluid Sci. 1996:13(1):55–70.
- [2] Ko T, Wu C. A numerical study on entropy generation induced by turbulent forced convection in curved rectangular ducts with various aspect ratios. Int Commun Heat Mass Transf. 2009;36(1):25–31.
- [3] You Y, Fan A, Liang Y, Jin S, Liu W, Dai F. Entropy generation analysis for laminar thermal augmentation with conical strip inserts in horizontal circular tubes. Int J Therm Sci. 2015;88:201–14.
- [4] Mwesigye A, Bello-Ochende T, Meyer JP. Heat transfer and entropy generation in a parabolic trough receiver with wall-detached twisted tape inserts. Int J Therm Sci. 2016;99:238–57.

- [5] Siavashi M, Bordbar V, Rahnama P. Heat transfer and entropy generation study of non-Darcy double-diffusive natural convection in inclined porous enclosures with different source configurations. Appl Therm Eng. 2017;110:1462–75.
- [6] Farzaneh-Gord M, Ameri H, Arabkoohsar A. Tube-in-tube helical heat exchangers performance optimization by entropy generation minimization approach. Appl Therm Eng. 2016;108:1279–87.
- [7] Chen B-S, Liu C-C. Heat transfer and entropy generation in fullydeveloped mixed convection nanofluid flow in vertical channel. Int J Heat Mass Transf. 2014;79:750–8.
- [8] Anand V. Entropy generation analysis of laminar flow of a nanofluid in a circular tube immersed in an isothermal external fluid. Energy. 2015;93:154–64.
- [9] Huminic G, Huminic A. Heat transfer and entropy generation analyses of nanofluids in helically coiled tube-in-tube heat exchangers. Int Commun Heat Mass Transf. 2016;71:118–25.
- [10] Ebrahimi A, Rikhtegar F, Sabaghan A, Roohi E. Heat transfer and entropy generation in a microchannel with longitudinal vortex generators using nanofluids. Energy. 2016;101:190–201.
- [11] Moghaddami M, Mohammadzade A, Esfehani SAV. Second law analysis of nanofluid flow. Energy Convers Manag. 2011;52(2):1397–405.
- [12] Keklikcioglu O, Ozceyhan V. Entropy generation analysis for a circular tube with equilateral triangle cross sectioned coiled-wire inserts. Energy. 2017;139:65–75.
- [13] Bejan A. Entropy generation minimization: The new thermodynamics of finite-size devices and finite-time processes. J Appl Phys. 1996;79(3):1191–218.
- [14] Ali S, Eidan A, Al-Sahlani A, Alshukri M, Ahmad A. The effect of vibration pulses on the thermal performance of evacuated tube heat pipe solar collector. J Mech Eng Res Dev. 2020;43:340–7.
- [15] Alsabery AI, Alshukri MJ, Jabbar NA, Eidan AA, Hashim I. Entropy generation and mixed convection of a nanofluid in a 3D wave tank with rotating inner cylinder. Energies. 2022;16(1):244.
- [16] Dagdevir T, Keklikcioglu O, Ozceyhan V. Heat transfer performance and flow characteristic in enhanced tube with the trapezoidal dimples. Int Commun Heat Mass Transf. 2019;108:104299.
- [17] Rashidi S, Zade NM, Esfahani JA. Thermo-fluid performance and entropy generation analysis for a new eccentric helical screw tape insert in a 3D tube. Chem Eng Process: Process Intensif. 2017;117:27–37.
- [18] Demir H, Dalkilic A, Kürekci N, Duangthongsuk W, Wongwises S. Numerical investigation on the single phase forced convection heat transfer characteristics of TiO2 nanofluids in a double-tube counter flow heat exchanger. Int Commun Heat Mass Transf. 2011;38(2):218–28.
- [19] Akhtari M, Haghshenasfard M, Talaie M. Numerical and experimental investigation of heat transfer of α -Al2O3/water nanofluid in double pipe and shell and tube heat exchangers. Numer Heat Transfer Part A: Appl. 2013;63(12):941–58.
- [20] Hamad RF, Alshukri MJ, Eidan AA, Alsabery AI. Numerical investigation of heat transfer augmentation of solar air heater with attached and detached trapezoidal ribs. Energy Rep. 2023;10:123–34.
- [21] Ya C, Ghajar A, Ma H. Heat and mass transfer fundamentals & applications. New York: McGraw-Hill; 2015.
- [22] Zimparov VD, Vulchanov NL. Performance evaluation criteria for enhanced heat transfer surfaces. Int J heat mass Transf. 1994;37(12):1807–16.
- [23] Keklikcioğlu O. İçerisinde grafen katkılı nanoakışkan ve konik iç eleman kullanılan boruda termohidrolik performans ve entropi üretiminin incelenmesi; 2020.